(Supplementary figure legends)

Figure S1. Experimental protocol of UVB-induced skin pigmentation in guinea pigs.

(A) Chemical structure of QNT 3-80. (B) Dorsal skins of guinea pigs were topically treated with QNT 3-80 (0.03-0.1%) and concurrently irradiated with UVB (350 mJ/cm^2 per exposure). Skin pigmentation was measured at 1 week after ending UVB radiation.

Figure S2. Effect of QNT 3-80 on cAMP-induced melanin production.

B16 cells were stimulated with forskolin (A), IBMX (B) or db-cAMP (C, D) for 3 days in the presence of QNT 3-80 or other sample. Melanin contents were measured with synthetic melanin as a standard and normalized to the cell numbers, representing as melanin pg/cell (A-C) or inhibition % (D). (E) B16 cells were incubated with QNT 3-80 for 3 days in the absence or presence of α-MSH. Cell viability was measured by MTT method, representing as absorbance values at 590 nm (A_{590}). Data are mean ± SD from three to five independent experiments. $^{\#}P < 0.05$ vs. media alone-added group. $*P < 0.05$ vs. α-MSH, IBMX or db-cAMP alone-stimulated group.

Figure S3. Effect of QNT 3-80 on UVB-induced skin pigmentation.

Dorsal skins of guinea pigs were topically treated with vehicle, QNT 3-80 or arbutin, and concurrently irradiated with UVB as described in the Method section. Groups of five animals were used in this experiment. (A) A representative photograph of the

pigmented skins. (B) Skin pigmentation was measured by using chromometer and is represented as a relative whitening (L) index with normal skin L = 10. $^{\#}P < 0.05$ vs. normal skin without UVB radiation. $*P < 0.05$ vs. UVB plus vehicle alone-applied group. (C) QNT 3-80 or other sample was dissolved in 100% ethyl alcohol and measured absorbance values at 200-400 nm.

Figure S4. Effects of QNT 3-80 on the α-MSH binding to its receptor and the forskolin-induced cAMP production.

(A) B16 cells were incubated with the fluorescent probe α-MSH, TAMRA-NDP-α-MSH (500 nM), for 2 h in the presence of QNT 3-80. After washing, the cells were subjected to flow cytometric analysis. (B) B16 cells were pretreated with QNT 3-80 for 2 h and stimulated with forskolin for 10-20 min in the presence of QNT 3-80. Cell extracts were subjected to ELISA to determine cAMP levels and normalized to the protein contents. Data are mean ± SD from three independent experiments. $^{\#}P < 0.05$ vs. media alone-added group.

Figure S5. Effect of QNT 3-80 on protein levels of PKA-Cα or PKA-RIIβ.

B16 cells were pretreated with QNT 3-80 for 2 h and stimulated with α-MSH for 20-30 min in the presence of QNT 3-80. Cell extracts were subjected to Western blot analysis (WB) with anti-PKA-RIIβ, anti-PKA-Cα or anti-GAPDH antibody.

Figure S6. Competition between QNT 3-80 and 8-[φ-575]-cAMP in the binding to PKA-RIIβ.

PKA-RIIβ polypeptide was pretreated with QNT 3-80 or Rp-cAMPS in cell-free reactions for 2 h, and incubated with the fluorescent probe 8-[φ-575]-cAMP at excess concentrations of up to 10-fold (10X) starting from 1X (1 μM) for another 2 h. 8-[φ-575]-cAMP binding to PKA-RIIβ polypeptide was measured as relative fluorescence units (RFU) under excitation at 575 nm and emission at 620 nm. Data are mean ± SD from three independent experiments. *P < 0.05 vs. 8-[φ-575]-cAMP (1X) plus QNT 3-80 alone-treated group or 8-[φ-575]-cAMP (1X) plus Rp-cAMPS alone-treated group.

Figure S7. Superimposed docking of QNT 3-80 onto the cAMP bound with PKA-RIIβ.

Docking arrangements of QNT 3-80 to the crystal structure of cAMP-binding A or B site of human PKA-RIIβ were carried out using the Surflex-Dock program, and superimposed onto those of the endogenous ligand cAMP. QNT 3-80 or its interacting residues on PKA-RIIβ is represented by a grey color, cAMP by a pink color, and the other PKA-RIIβ backbone by a green color. Hydrogen bonding between QNT 3-80 and PKA-RIIβ is shown as a black dotted line.

Figure S8. Effect of QNT 3-80 on tyrosinase expression.

B16 cells were pretreated with QNT 3-80 or Rp-cAMPS for 2 h and stimulated with α-MSH for 48 h (A) or 12 h (B) in the presence of QNT 3-80 or Rp-cAMPS. (A) Cell extracts were subjected to Western blot analysis (WB) with anti-tyrosinase or anti-GAPDH antibody. (B) Total RNAs were subjected to RT-PCR analysis of tyrosinase with the internal control β-actin. (C) B16 cells were transfected with Tyrosinase (-2236/+59)-Luc reporter construct in combination with *Renilla* control vector, and then stimulated with α-

MSH for 20 h in the presence of QNT 3-80. Cell extracts were subjected to a dual-luciferase assay. Firefly luciferase activity is represented as a relative fold after normalizing to the *Renilla* activity. Data are mean ± SD from three independent experiments. $^{\#}P < 0.05$ vs. media alone-added group. $*P < 0.05$ vs. α-MSH alone-stimulated group. Dorsal skins of guinea pigs were topically treated with QNT 3-80 and concurrently irradiated with UVB as described in the Method section. Skin tissues were biopsied. (D) Cell extracts were subjected to WB with anti-tyrosinase or anti-GAPDH antibody. (E) Total RNAs were subjected to RT-PCR analysis of tyrosinse with the internal control β-actin.

Figure S9. Effects of QNT 3-80 on the copper ion chelation and the tyrosinase activity.

(A) QNT 3-80 (50 μM) was dissolved in 100% ethyl alcohol, reacted with variable concentrations (0-50 μM) of $CuSO_4$, and then measured absorbance values at 200-400 nm. Mushroom tyrosinase (B) or human tyrosinase (C) was treated with QNT 3-80 or arbutin in cell-free reactions for 10 min, and its catalytic activity was then determined as L-tyrosine oxidation velocity. Data are mean ± SD from three independent experiments. $*P < 0.05$ vs. tyrosinase alone-containing group.

Supplementary Figure S1

A

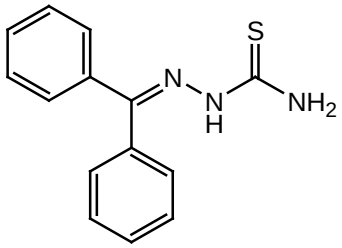

B

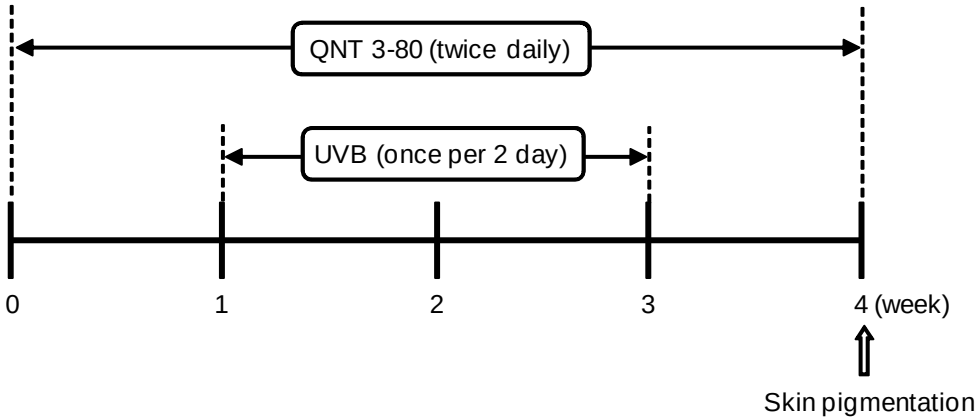

Supplementary Figure S2

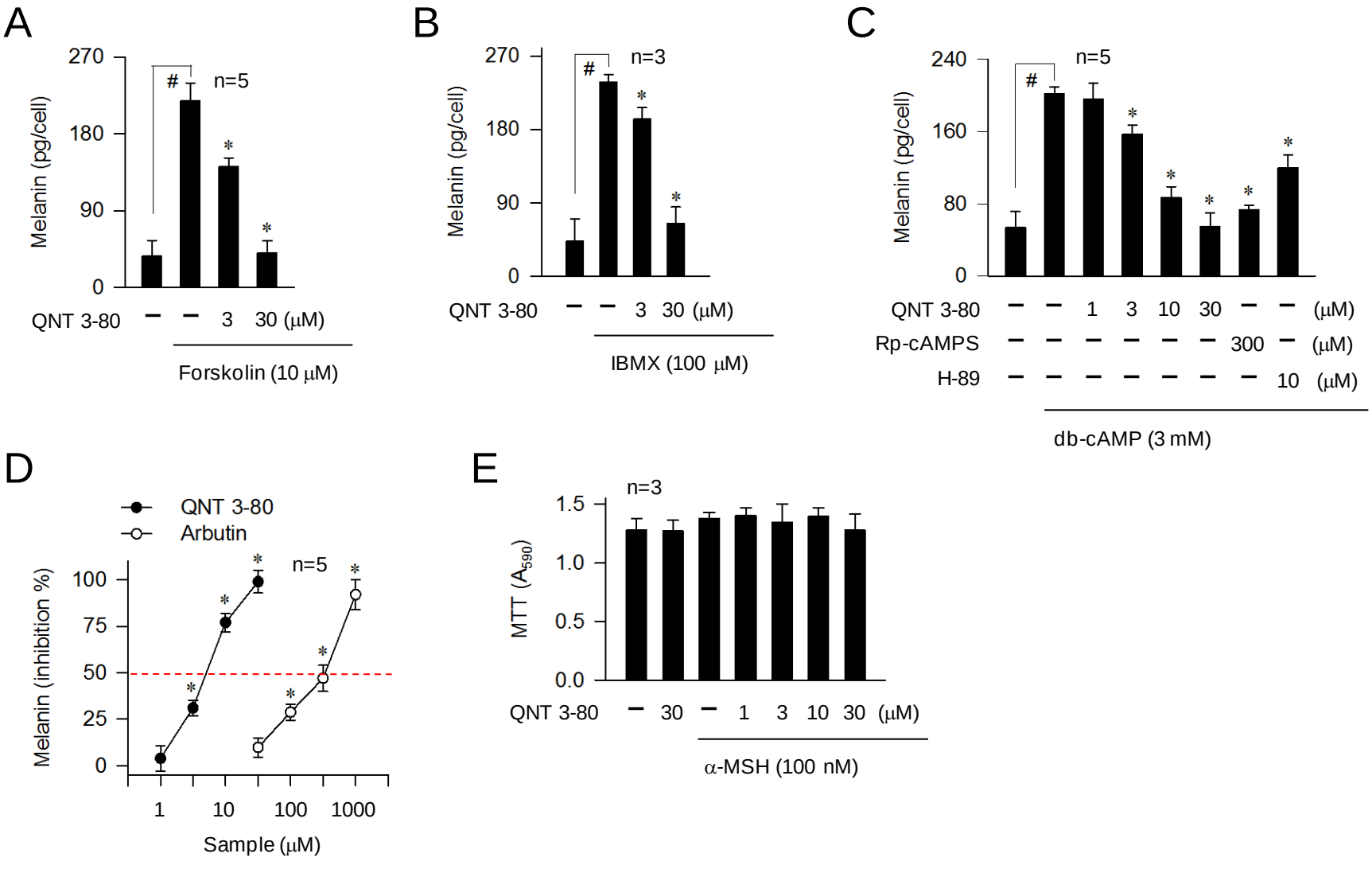

Supplementary Figure S3

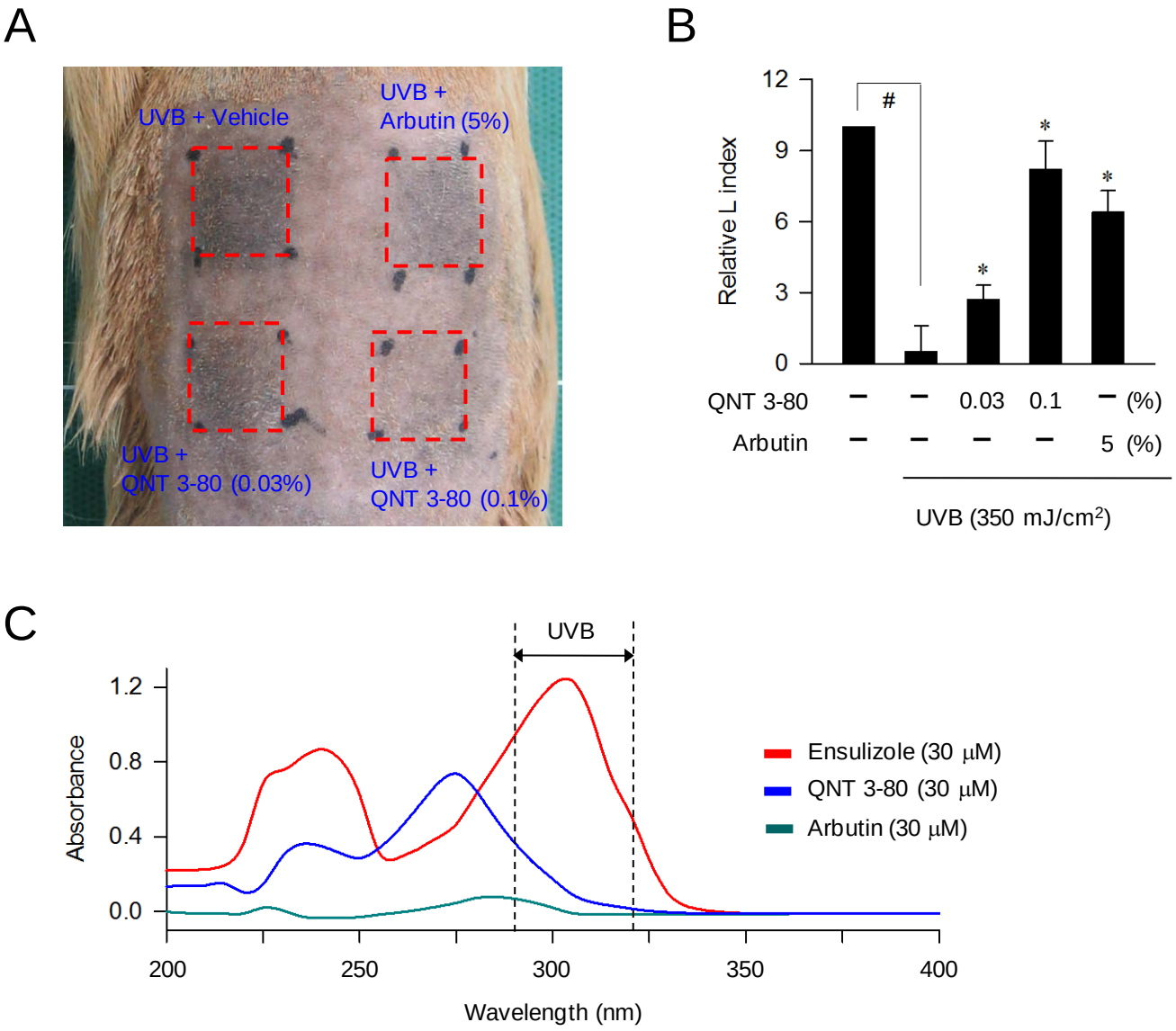

Supplementary Figure S4

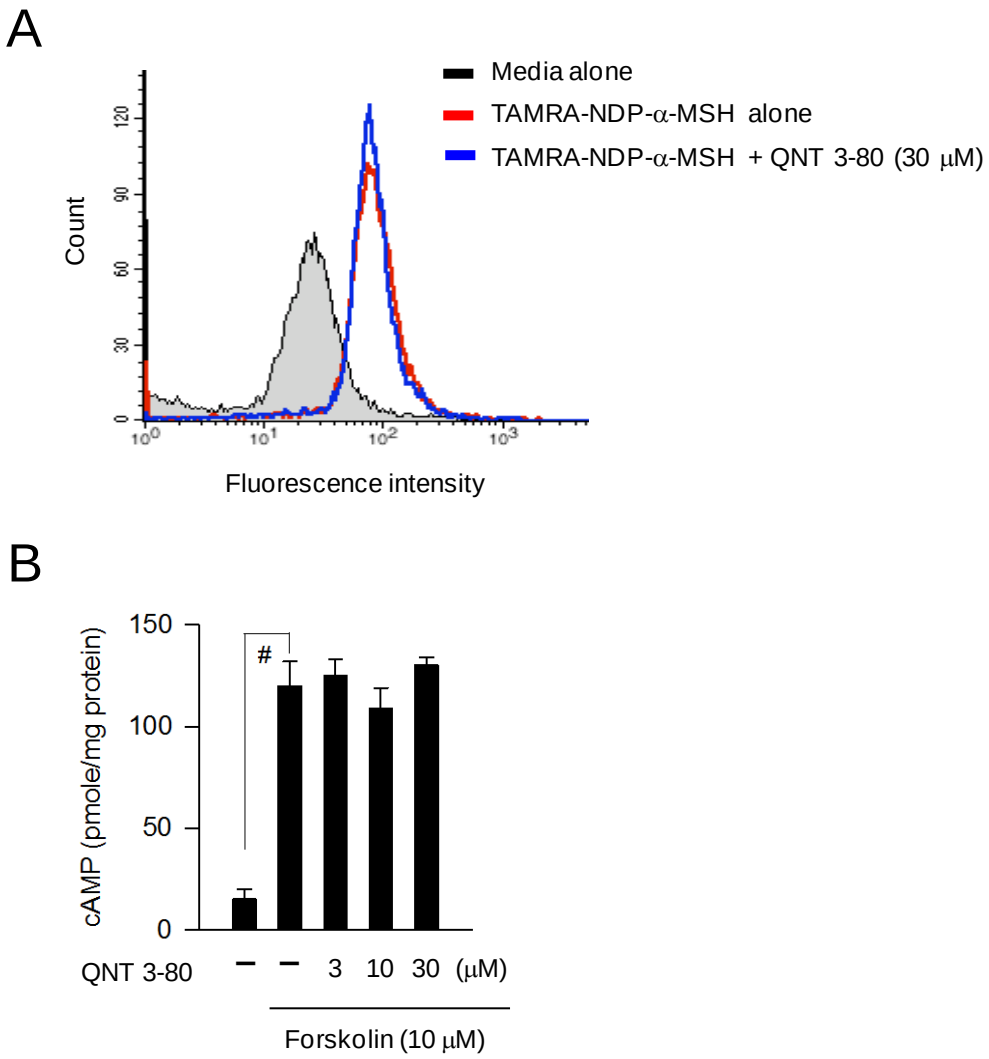

Supplementary Figure S5

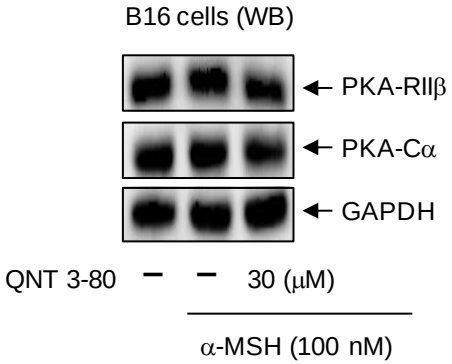

Supplementary Figure S6

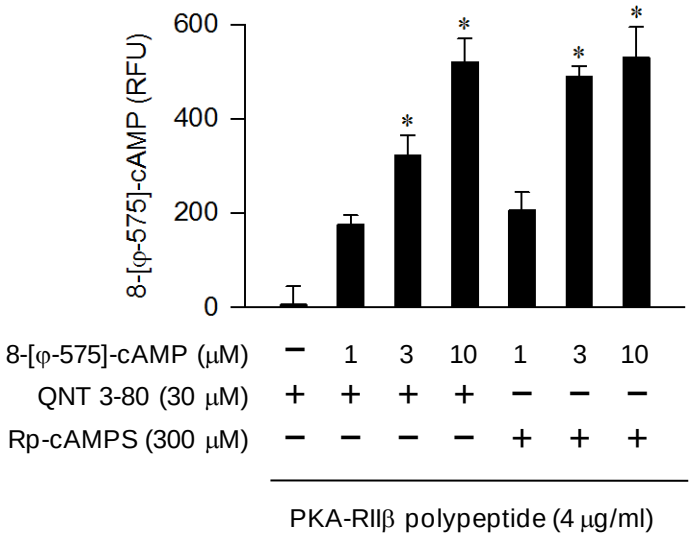

Supplementary Figure S7

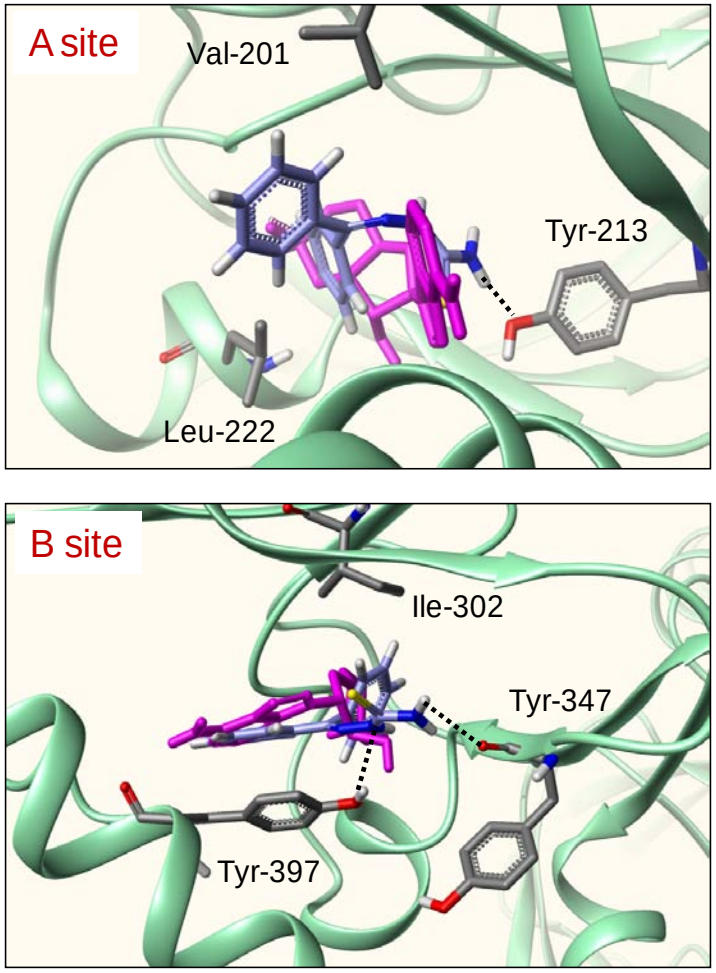

Supplementary Figure S8

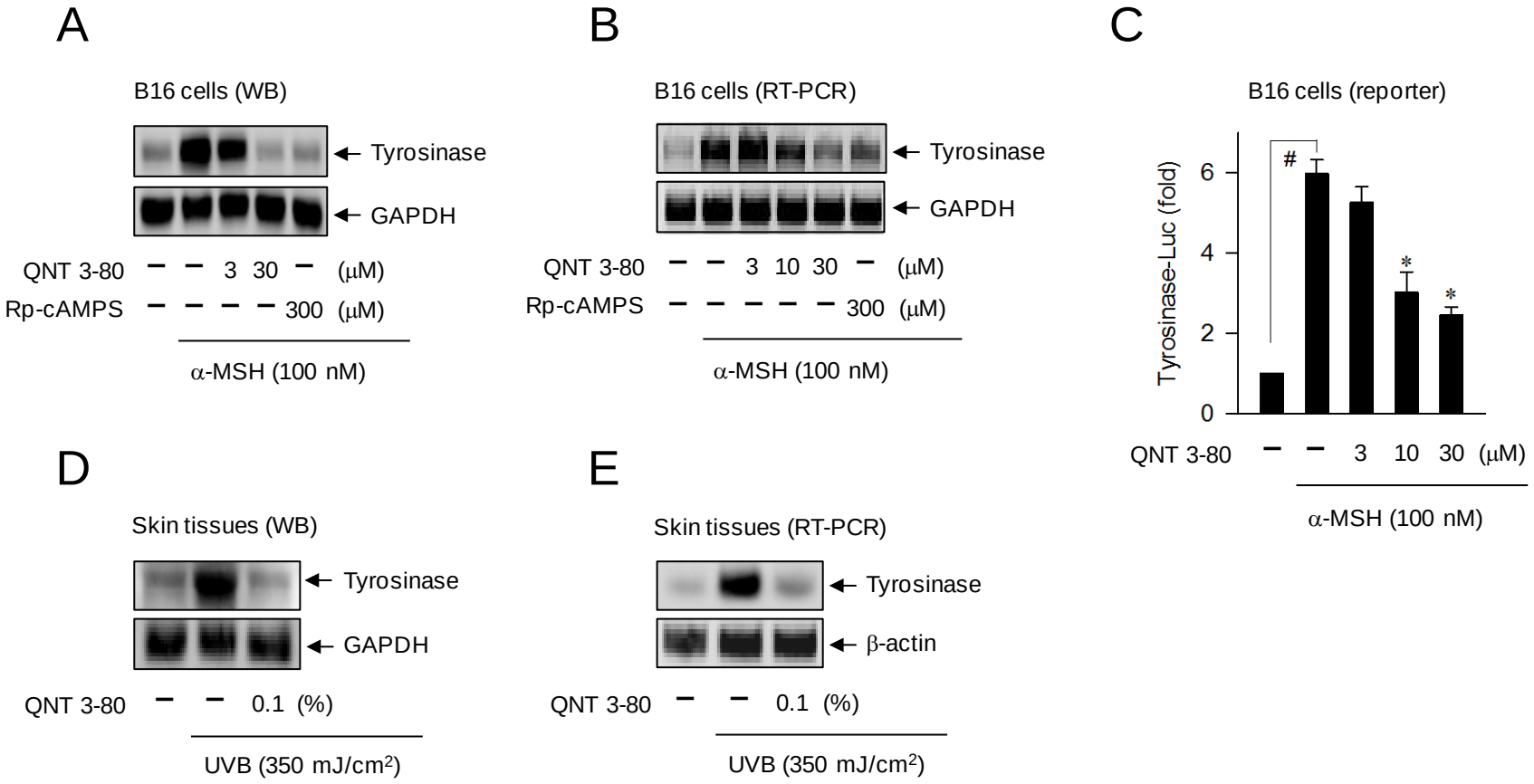

Supplementary Figure S9